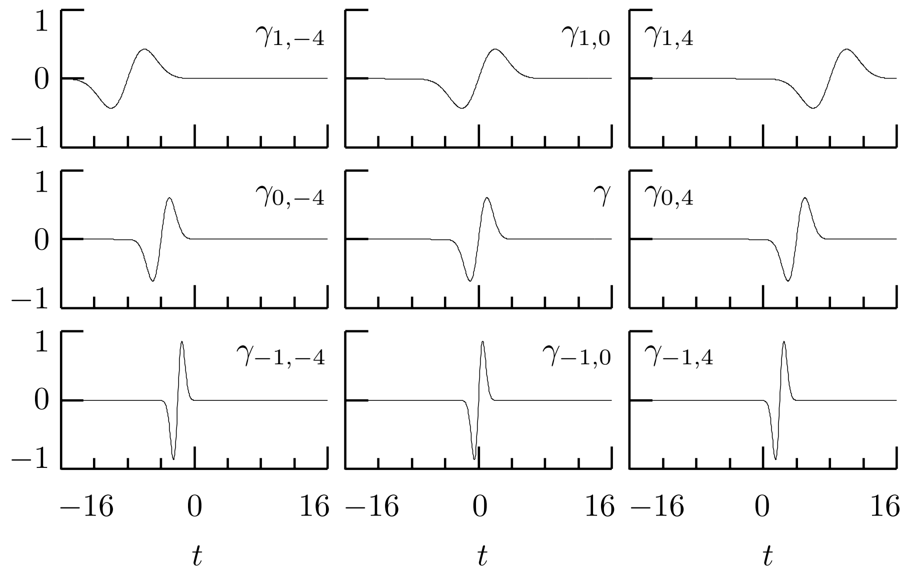

Figure 458. Translation and dilation of the function defined by $\gamma(t) = t\exp(-t^2/2)$.

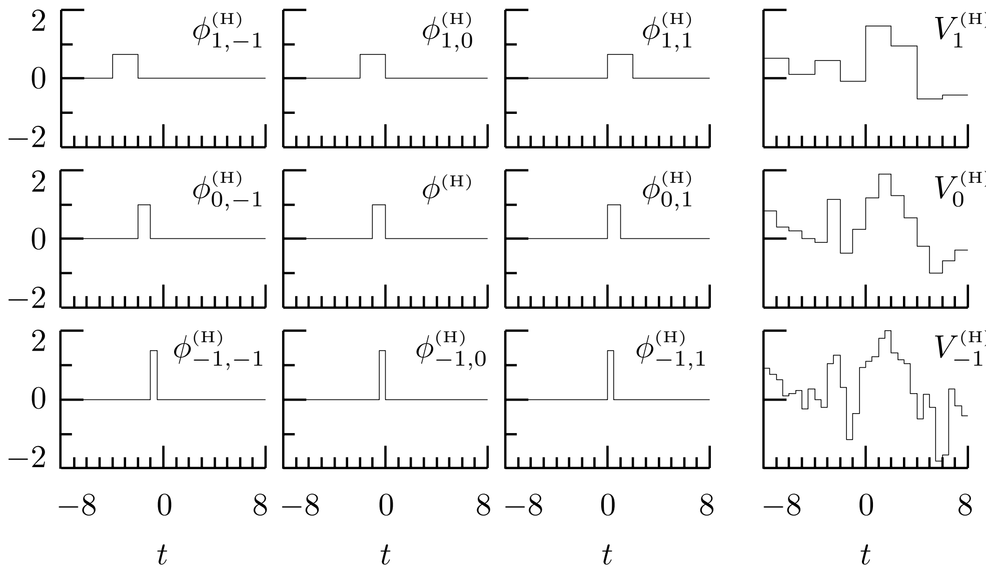

Figure 461. The Haar scaling function $\phi^{(\mathrm{H})}(\cdot)$ and corresponding approximation spaces. The first three plots on the middle row show three of the basis functions for the Haar approximation space $V_0^{(\mathrm{H})}$, namely, from left to right, $\phi_{0,-1}^{(\mathrm{H})}(\cdot)$, $\phi^{(\mathrm{H})}(\cdot)$ and $\phi_{0,1}^{(\mathrm{H})}(\cdot)$. The right-most plot on this row is an example of a function contained in $V_0^{(\mathrm{H})}$. The top and bottom rows show, respectively, corresponding plots for the Haar approximation spaces $V_1^{(\mathrm{H})}$ (a coarser approximation than $V_0^{(\mathrm{H})}$) and $V_{-1}^{(\mathrm{H})}$ (a finer approximation than $V_0^{(\mathrm{H})}$). The right-most column of plots can be regarded as three Haar approximations of a single $L^2(\mathbb{R})$ function, with the associated scales of 2, 1 and 1/2 (top to bottom).

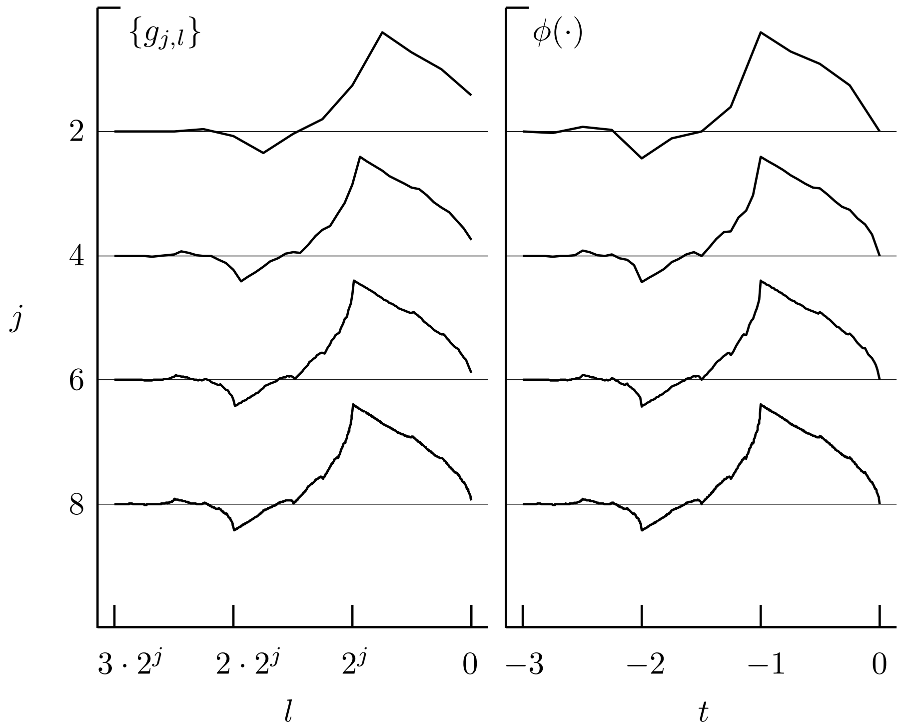

Figure 471. Level j equivalent D(4) scaling filters $\{g_{j,l}\}$ (left-hand column) and the D(4) scaling function $\phi(\cdot)$ evaluated over the grid defined by $\frac{l}{2^j}$, $l = -3 \cdot 2^j, \ldots, -1, 0$ (right-hand) for $j = 2, 4, 6$ and 8 (top to bottom). For a given j, the two plotted sequences consist of $3 \cdot 2^j + 1$ values connected by line segments. In the right-hand column, the function $\phi(\cdot)$ is plotted at values $t = -3.0$ to $t = 0$ in steps of, from top to bottom, 0.25, 0.0625, 0.015625 and 0.00390625. The filters in the left-hand column are plotted in such a manner as to illustrate the approximation of Equation (469), whose validity increases with increasing j.

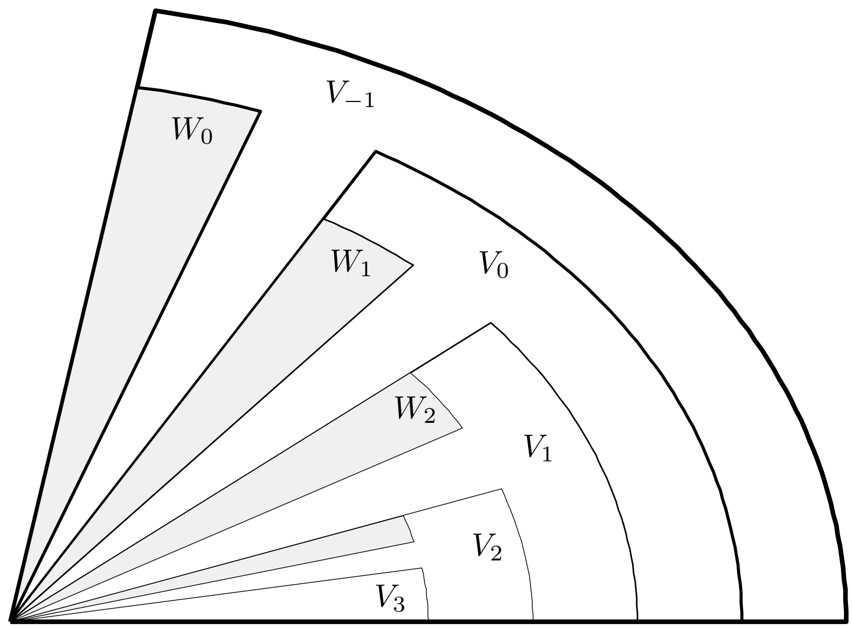

Figure 473a. Venn diagram illustrating the nesting of subspaces V_j and W_j. There are five arcs emanating from the baseline. Starting at each end of an arc, there is a line segment that continues to the lower left-hand corner of the plot. The area enclosed by a given arc and the two line segments emanating from its ends represents an approximation space V_j. The largest such area outlines the entire figure and represents V_{-1}, while the smallest area represents V_3 (note that $V_3 \subset V_2 \subset V_1 \subset V_0 \subset V_{-1}$, as required). The shaded areas represent the detail spaces W_j. Note that $W_0 \subset V_{-1}$, $W_1 \subset V_0$, $W_2 \subset V_1$ and $W_3 \subset V_2$ (there is no label for W_3 due to lack of space). Note also that, while $V_0 \subset V_{-1}$ and $W_0 \subset V_{-1}$, it is the case that $V_0 \cup W_0 \neq V_{-1}$ because V_{-1} also contains linear combinations of functions that are in both V_0 and W_0 – such linear combinations need not be in either V_0 or W_0, but rather can be in the space disjoint to V_0 and W_0 and represented by the scythe-like shape bearing the label V_{-1}. Finally, note that all the V_j and W_j intersect at a single point (represented by the lower left-hand corner of the plot) because all these spaces must contain the null function.

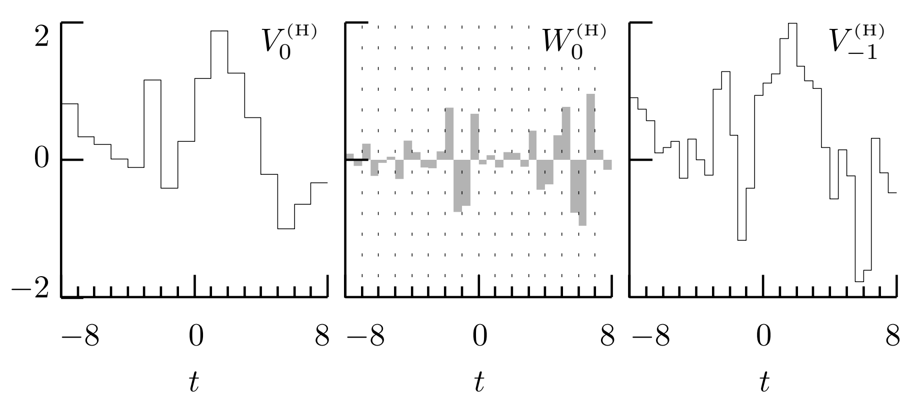

Figure 473b. Examples of functions in $V_0^{(\mathrm{H})}$, $W_0^{(\mathrm{H})}$ and $V_{-1}^{(\mathrm{H})}$. Note that, while the function in $V_0^{(\mathrm{H})}$ is constant over intervals of the form $(k-1, k]$ for $k \in \mathbb{Z}$, the function in $W_0^{(\mathrm{H})}$ integrates to zero over such intervals (the ends of these intervals are indicated in the middle plot by the vertical dotted lines). The function in $V_{-1}^{(\mathrm{H})}$ is in fact formed by point-wise addition of the functions in the other two spaces.

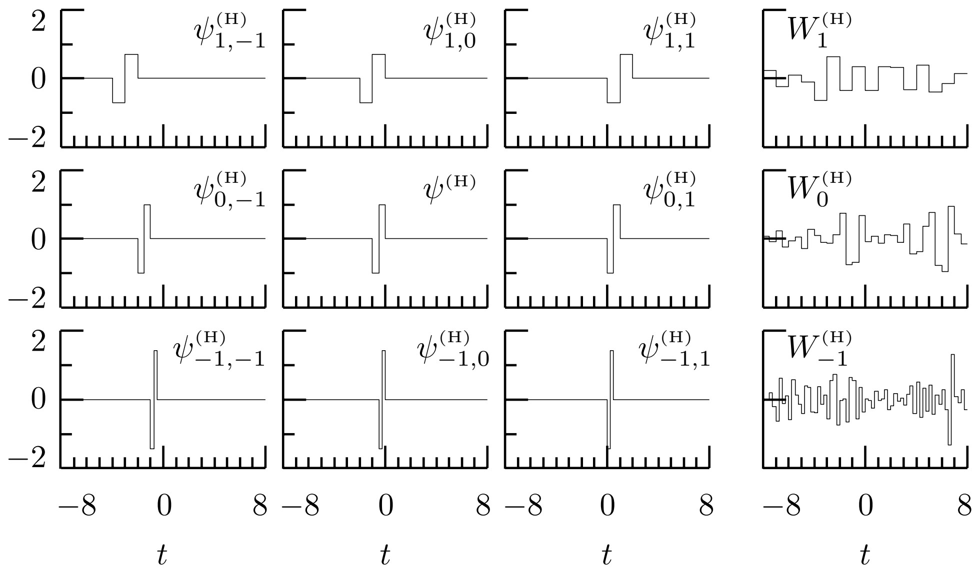

Figure 475. The Haar wavelet function $\psi^{(H)}(\cdot)$ and corresponding detail spaces. The first three plots on the middle row shows three of the basis functions for the Haar detail space $W_0^{(H)}$, namely, from left to right, $\psi^{(H)}_{0,-1}(\cdot)$, $\psi^{(H)}(\cdot)$ and $\psi^{(H)}_{0,1}(\cdot)$. The right-most plot on this row is an example of a function contained in $W_0^{(H)}$. The top and bottom rows show, respectively, corresponding plots for the Haar detail spaces $W_1^{(H)}$ and $W_{-1}^{(H)}$ (Figure 461 shows the corresponding Haar scaling function and approximation spaces).

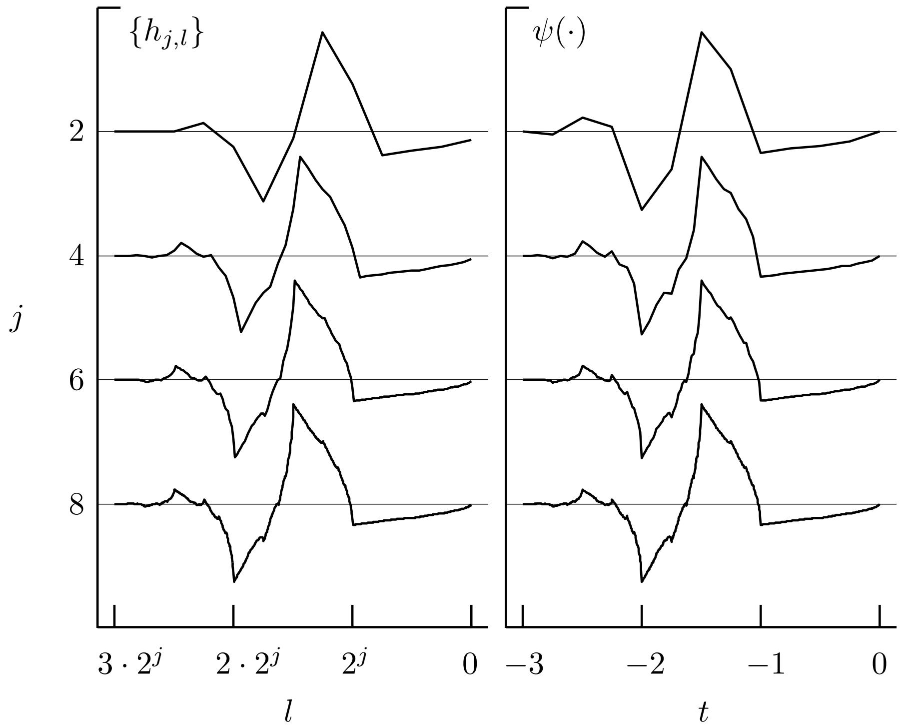

Figure 478. Level j equivalent D(4) wavelet filters $\{h_{j,l}\}$ (left-hand column) and the D(4) wavelet function $\psi(\cdot)$ evaluated over the grid defined by $\frac{l}{2^j}$, $l = -3 \cdot 2^j, \ldots, -1, 0$ (right-hand) for $j = 2, 4, 6$ and 8 (top to bottom). For details on the layout, see the caption for the analogous Figure 471.

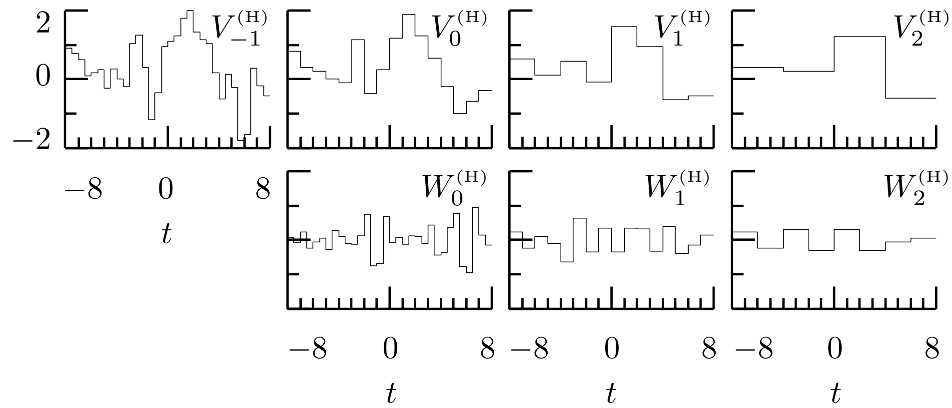

Figure 482. Multiresolution analysis of a function $x(\cdot) \in V_{-1}^{(H)}$ (upper left-hand plot), yielding three approximations, namely, $s_0(\cdot) \in V_0^{(H)}$, $s_1(\cdot) \in V_1^{(H)}$ and $s_2(\cdot) \in V_2^{(H)}$ (remaining plots on top row, from left to right), along with corresponding details $d_0(\cdot) \in W_0^{(H)}$, $d_1(\cdot) \in W_1^{(H)}$ and $d_2(\cdot) \in W_2^{(H)}$ (bottom row, from left to right).

$h_l \equiv \bar{h}_{-l},\ l = 0, \ldots, L-1$	$g_l \equiv \bar{g}_{-l},\ l = 0, \ldots, L-1$
$\bar{h}_l = (-1)^l \bar{g}_{1-l-L}$	$\bar{g}_l \equiv (-1)^{l+1} \bar{h}_{1-l-L}$
$\{\bar{h}_l\} \longleftrightarrow \overline{H}(\cdot)$	$\{\bar{g}_l\} \longleftrightarrow \overline{G}(\cdot)$
$\{h_l\} \longleftrightarrow H(\cdot)$	$\{g_l\} \longleftrightarrow G(\cdot)$
$H(f) = \overline{H}(-f)$	$G(f) = \overline{G}(-f)$
$\overline{H}(0) = 0$	$\overline{G}(0) = \sqrt{2}$
$\overline{H}(f) = -e^{i2\pi f(L-1)}\overline{G}(\frac{1}{2} - f)$	$\overline{G}(f) = e^{i2\pi f(L-1)}\overline{H}(\frac{1}{2} - f)$
$\overline{H}^{(m)}(0) = 0,\ m = 0, \ldots, r-1$	$\overline{G}^{(m)}(\frac{1}{2}) = 0,\ m = 0, \ldots, r-1$
$\bar{h}_l = \int \phi(t-l)\frac{\psi(\frac{t}{2})}{\sqrt{2}}\, dt$	$\bar{g}_l = \int \phi(t-l)\frac{\phi(\frac{t}{2})}{\sqrt{2}}\, dt$
$\int \psi(t) dt = 0$	$\int \phi(t)\, dt = 1$
support $\{\psi(\cdot)\} \subset (-(L-1), 0]$	support $\{\phi(\cdot)\} \subset (-(L-1), 0]$
$\psi(\cdot) \longleftrightarrow \Psi(\cdot)$	$\phi(\cdot) \longleftrightarrow \Phi(\cdot)$
$\Psi(-2^j f) \approx \widetilde{H}_j(f)$	$\Phi(-2^j f) \approx \widetilde{G}_j(f)$
$\psi(-\frac{l}{2^j}) \approx 2^j \tilde{h}_{j,l} = 2^{j/2} h_{j,l}$	$\phi(-\frac{l}{2^j}) \approx 2^j \tilde{g}_{j,l} = 2^{j/2} g_{j,l}$
$\Psi(f) = \Phi(\frac{f}{2})\frac{\overline{H}(\frac{f}{2})}{\sqrt{2}}$	$\Phi(f) = \Phi(\frac{f}{2})\frac{\overline{G}(\frac{f}{2})}{\sqrt{2}}$
$\Psi(f) = \frac{\overline{H}(\frac{f}{2})}{\sqrt{2}} \prod_{m=2}^{\infty} \frac{\overline{G}(\frac{f}{2^m})}{\sqrt{2}}$	$\Phi(f) = \prod_{m=1}^{\infty} \frac{\overline{G}(\frac{f}{2^m})}{\sqrt{2}}$
$\psi_{j,k}(t) \equiv \psi(\frac{t}{2^j} - k)/\sqrt{2^j}$	$\phi_{j,k}(t) \equiv \phi(\frac{t}{2^j} - k)/\sqrt{2^j}$
$\psi(t) = \sqrt{2}\sum_l \bar{h}_l \phi(2t - l)$	$\phi(t) = \sqrt{2}\sum_l \bar{g}_l \phi(2t - l)$
$w_{j,k} = \int x(t)\psi_{j,k}(t)\, dt$	$v_{j,k} = \int x(t)\phi_{j,k}(t)\, dt$
$w_{j,k} = \sum_l h_l v_{j-1,2k-l}$	$v_{j,k} = \sum_l g_l v_{j-1,2k-l}$

Table 499. Key relationships involving (i) wavelet and scaling filters $\{h_l\}$ and $\{g_l\}$ and their time reverses $\{\bar{h}_l\}$ and $\{\bar{g}_l\}$ and (ii) wavelet functions $\psi(\cdot)$ and scaling functions $\phi(\cdot)$.